OXFORD GENETICS

GENETICS, 2022, 221(3), iyac075
https://doi.org/10.1093/genetics/iyac075
Advance Access Publication Date: 10 May 2022
Investigation

Translational suppression via IFG-1/eIF4G inhibits stress-induced RNA alternative splicing in *Caenorhabditis elegans*

Samantha C. Chomyshen,[1] Hadi Tabarraei,[1] Cheng-Wei Wu [1,2,3,*]

[1]Department of Veterinary Biomedical Sciences, Western College of Veterinary Medicine, University of Saskatchewan, Saskatoon, SK S7N 5B4, Canada,
[2]Toxicology Centre, University of Saskatchewan, Saskatoon, SK S7N 5B3, Canada,
[3]Department of Biochemistry, Microbiology and Immunology, College of Medicine, University of Saskatchewan, Saskatoon, SK S7N 5E5, Canada

*Corresponding author: Department of Veterinary Biomedical Sciences, Western College of Veterinary Medicine, University of Saskatchewan, Saskatoon, SK S7N 5B4, Canada. Email: michael.wu@usask.ca

Abstract

Splicing of precursor mRNA is an essential process for dividing cells, and splicing defects have been linked to aging and various chronic diseases. Environmental stress has recently been shown to modify alternative splicing, and molecular mechanisms that influence stress-induced alternative splicing remain unclear. Using an in vivo RNA splicing reporter, we performed a genome-wide RNAi screen in *Caenorhabditis elegans* and found that protein translation suppression via silencing of the conserved eukaryotic initiation factor 4G (IFG-1/eIF4G) inhibits cadmium-induced alternative splicing. Transcriptome analysis of an *ifg-1*-deficient mutant revealed an overall decrease in intronic and intergenic reads and prevented cadmium-induced alternative splicing compared to the wild type. We found that the *ifg-1* mutant up-regulates >80 RNA splicing regulatory genes controlled by the TGF-β transcription factor SMA-2. The extended lifespan of the *ifg-1* mutant is partially reduced upon *sma-2* depletion and completely nullified when core spliceosome genes including *snr-1*, *snr-2*, and *uaf-2* are knocked down. Depletion of *snr*-1 and *snr-2* also diminished the enhanced cadmium resistance of the *ifg-1* mutant. Together, these data describe a molecular mechanism through which translation suppression inhibits stress-induced alternative splicing and demonstrate an essential role for RNA splicing in promoting longevity and stress resistance in a translation-compromised mutant.

Keywords: RNA splicing; aging; environmental stress

Introduction

Posttranscriptional splicing of precursor mRNAs (pre-mRNA) is an essential step in the regulation of eukaryotic gene expression and contributes to proteome diversity (Baralle and Giudice 2017). Precision in RNA splicing is necessary for maintaining cellular homeostasis; this includes alternative splicing of select transcripts into isoform variants in specific tissues, or in response to particular developmental cues to coordinate organismal growth (Wang *et al.* 2008; Nilsen and Graveley 2010). Errors in RNA splicing can disrupt cellular homeostasis, driven by the assembly of aberrant mRNA molecules that lead to the production of erroneous proteins with abnormal functions and detrimental consequences (Dutertre *et al.* 2011). A decline in RNA splicing fidelity has been reported during aging and is prominently linked to many chronic human diseases including neurodegeneration and cancer (Tollervey *et al.* 2011; Scotti and Swanson 2016; Deschênes and Chabot 2017). However, underlying cellular mechanisms that influence splicing fidelity remains poorly understood. Uncovering mechanistic insights into alternative splicing regulation is intriguing as small molecules that modulate RNA splicing have been explored for their potential as chemotherapy agents (Eskens *et al.* 2013).

In the genetic model *Caenorhabditis elegans*, it was recently demonstrated that RNA splicing fidelity deteriorates with age and this dysregulation is hypothesized to be a central contributor to the decline in transcriptome and protein homeostasis (Heintz *et al.* 2017). Interventions that extend lifespan such as dietary restriction can improve splicing fidelity during aging; conversely, loss of splicing homeostasis nullifies dietary restriction-induced longevity, suggesting a codependency of dietary restriction and splicing homeostasis in extending lifespan. In Rhesus monkeys, caloric restriction extends lifespan and leads to modifications of RNA splicing as evident by the up-regulation of various spliceosome components at the transcriptome and proteome levels in the liver (Rhoads *et al.* 2018). This suggests that a causative relationship between RNA homeostasis and dietary restriction-induced longevity in *C. elegans* may be conserved in higher organisms. Next to dietary restriction, other interventions that significantly extend *C. elegans* lifespan include reduced insulin and TOR signaling (Kenyon *et al.* 1993; Robida-Stubbs *et al.* 2012), decreased mitochondrial respiration (Felkai *et al.* 1999; Feng *et al.* 2001), and inhibition of protein translation (Hansen *et al.* 2007; Pan *et al.* 2007); however, whether maintaining RNA splicing is essential for the longevity phenotype of these interventions remain to be characterized.

Received: March 11, 2022. **Accepted:** April 22, 2022

Recently, we showed that RNA splicing is disrupted in *C. elegans* upon exposure to the heavy metal cadmium (Wu *et al.* 2019). This demonstrated that environmental stress may promote aging by negatively influencing RNA homeostasis. In this study, we performed a genome-wide RNAi screen and found that knockdown of protein translation via reduced translation initiation factor *ifg-1* (initiation factor 4G family) inhibits cadmium-induced alternative splicing. This inhibitory effect is dependent on the transcription factor gene *sma-2*, which is required for the expression of >80 genes involved in RNA splicing that is up-regulated in the *ifg-1* mutant. Knockdown of select core RNA splicing regulators reduced the lifespan and cadmium survival of the *ifg-1* mutant, implicating an essential role for RNA splicing factors in promoting longevity and stress resistance of this translation compromised mutant. Overall, our results suggest a model where reduced protein translation up-regulates the expression of RNA splicing regulatory genes via the SMA transcription factors to modify alternative splicing under stress to promote longevity and stress resistance.

Materials and methods

C. elegans strains

C. elegans strains were grown and maintained at 20°C using standard methods (Brenner 1974). The following strains were used: wild-type N2 Bristol, KH2235 *lin-15(n765) ybIs2167[eft-3::ret-1E4E5(+1)E6-GGS6-mCherry+eft-3::ret-1E4E5(+1)E6(+2) GGS6-EGFP+lin-15(+)+pRG5271Neo]*X, *ifg-1(cxTi9279)*. The KX52 *ifg-1(cxTi9279) II; bcIs39 V* strain was used to isolate the *ifg-1(cxTi9279)* allele followed by 4 rounds of outcrossing with N2.

Genome-wide RNAi screen and RNAi experiments

RNAi was performed as described previously by feeding *C. elegans* strains of engineered *Escherichia coli [HT115(DE3)]* that transcribed double-stranded RNA (dsRNA) homologous to a target gene (Wu *et al.* 2016, 2019). Approximately 19,000 dsRNA from the ORFeome RNAi feeding library (Open Biosystems, Huntsville, AL, USA) and the MRC genomic RNAi feeding library (Geneservice, Cambridge, UK) were used for screening. Briefly, synchronized L1 larvae of KH2235 *C. elegans* obtained from the alkaline hypochlorite method were grown in liquid nematode growth medium (NGM) with dsRNA producing bacteria for 2 days, followed subsequently by exposure to 300 μM cadmium chloride for 24 h and manually screened for relative fluorescence of the *ret-1* GFP reporter under an Olympus SZX61 stereomicroscope. Clones that resulted in the retention of *ret-1* GFP signal after 24 h cadmium exposure were recorded and rescreened 3 additional times for verification. All subsequent RNAi experiments were performed on NGM agar plates in the presence of 50 μg mL^{-1} carbenicillin and 100 μg mL^{-1} isopropyl β-D-thiogalactopyranoside. *E. coli* expressing the pPD129.36 (LH4440) plasmid encoding 202 bases of dsRNA that are not homologous to any predicted *C. elegans* gene, or referred to as empty vector (EV), was used as an RNAi control.

RNA extraction and RT-PCR

Total RNA was extracted with the Invitrogen Purelink RNA mini kit (ThermoFisher, 12183020) according to the manufacturer's instructions using a QSonica Q55 sonicator. RNA was extracted from 4 biological replicates per condition, with each sample containing 200–300 synchronized worms. RNA samples were treated with DNAse I (ThermoFisher, EN0521) before cDNA synthesis using the Invitrogen Multiscribe reverse transcriptase (ThermoFisher, 4311235). Analysis of *ret-1* alternative splicing was carried out with primers previously described using the Applied Biosystems ProFlex thermocycler (Heintz *et al.* 2017). RT-PCR product was separated on a 2.5% agarose gel and stained with SYBR Green I nucleic acid gel stain (ThermoFisher, S7563) for band visualization using a BioRad Gel Doc EQ system.

Fluorescent microscopy

Preparation of *C. elegans* for fluorescent imaging was carried out as previously described (Murray *et al.* 2020). Fluorescent images were captured with a Retiga R3 camera mounted to a Zeiss Axioskop 50 microscope. GFP fluorescence was detected using filter sets with Ex: 460–495 nm/Ex: 510–550 nm and RFP fluorescence was detected using filter sets with Ex: 540–580 nm/Em: 610 nm. Grayscale images were converted to color images using ImageJ (Schneider *et al.* 2012). Worm images used to quantify relative fluorescence were prepared by mounting 8 worms per slide immobilized by 2% sodium azide on a 2% agarose pad. Relative fluorescence was calculated in ImageJ using the Measure function. Background signal was subtracted from each image by defining an area on the same image where fluorescence signal was absent, with the dimension of the defined background constant for all images. Composite images displaying both GFP and RFP fluorescence were created with the Merge Channel function in ImageJ.

Lifespan and cadmium survival assay

Lifespan assays were performed at 20°C on NGM RNAi plates seeded with HT115 *E. coli* with the EV dsRNA plasmid used for control. To circumvent the larval arrest phenotype of most RNAi tested in this study, synchronized L1 worms were first grown on EV dsRNA until day 1 of adulthood, after which the worms were transferred to RNAi plates seeded with the corresponding dsRNA to initiate knockdown of the gene of interest. For 2 dsRNA that did not affect larval development (*sma-2*, *sma-3*), RNAi was initiated at the L1 stage. Lifespan assays were performed without the use of FUDR with progeny separation accomplished via daily picking during the worm's reproductive window. For cadmium survival assay, synchronized L1 worms were first grown on EV dsRNA until day 1 of adulthood followed by transfer to RNAi plates seeded with the corresponding dsRNA for 48 h to initiate gene knockdown. Three-day-old worms were then transferred to corresponding RNAi seeded NGM plates containing 300 μM of cadmium chloride. For both lifespan and survival assays, worms were considered dead if they did not respond to gentle prodding with a metal pick and censored when they displayed protruding gonad or vulva. Survival assays were scored daily while lifespan assays were scored every 2 days. Three independent trials were performed for each assay, with the number of animals used in each experiment described in the corresponding supplementary table.

Whole-transcriptome sequencing and data analysis

Wild-type and *ifg-1(cxTi9279)* worms were synchronized at the L1 stage and grown on EV dsRNA NGM plates until day 1 of adulthood followed by transfer to EV dsRNA NGM plates with or without 300 μM of cadmium chloride for 24 h. Total RNA from wild-type and *ifg-1(cxTi9279)* worms with and without cadmium treatment were extracted from 3 biological replicates for each condition with ~2,000-3,000 worms per replicate. RNA samples were sent to Novogene (Sacramento, CA, USA) on dry ice for cDNA library

preparation with oligo(dT) enrichment followed by RNA-sequencing and statistical analysis. HISAT2 (v2.0.5) was used to map sequencing reads to the WBcel235 genome, with FeatureCounts (v1.5.0-p3) used for gene quantification, DESeq2 (v1.20.0) for differentially analysis, and rMATS (v3.2.5) for alternative splicing analysis (Anders and Huber 2010; Shen *et al.* 2014; Kim *et al.* 2019). Gene ontology enrichment was performed using DAVID functional analysis (Huang *et al.* 2009). Fold enrichment is shown that is defined as the ratio between observed (occurrence within the provided gene list) and expected (occurrence within the transcriptome) frequency of a given gene ontology term. Heat maps showing differentially expressed genes were analyzed using Gene Cluster 3.0 with uncentered average linkage and visualized with Java TreeView (v1.2.0). Raw sequence data and processed data are deposited to the NCBI Gene Expression Omnibus with the accession number GSE184491. Raw data from previously published RNA-sequencing of *sma-2(rax5)* and *sma-4(rax3)* were retrieved from the NCBI Sequence Read Archive with the BioProject ID PRJNA395096 (Yu *et al.* 2017). The Galaxy (usegalaxy.org) open-source platform was used to analyze differential gene expression data using the aforementioned methods (Afgan *et al.* 2018).

Measurement of motility

Wild-type and *ifg-1(cxTi9279)* worms were synchronized at the L1 stage and grown on EV dsRNA NGM plates until day 1 of adulthood followed by transfer to EV dsRNA NGM plates with or without 300 µM of cadmium chloride for 24 or 48 h. *C. elegans* swimming rate (body bends per second in liquid) was measured by re-suspending worms grown on a 6-cm NGM agar plate with ∼5 ml of M9 buffer. Worms were allowed to acclimate to the liquid condition for at least 1 min, after which the swimming behavior was recorded by a Retiga R3 camera mounted to an Olympus SZX61 stereomicroscope for 30 s. The video file was processed with the wrMTrck program in ImageJ to calculate body bends per second (Nussbaum-Krammer *et al.* 2015).

Statistical analyses

Graphical data and statistical analysis were generated using the GraphPad Prism software (v7.04). For statistical analysis, the Student's *t*-test was performed when 2 means were compared. One -way ANOVA with Tukey's correction was used for multiple comparisons with 1 factor, and 2-way ANOVA with Sidak correction was used for multiple comparisons with 2 factors. *F*-test for linear regression was used to determine statistical significance when comparing relationships between 2 sets of RNA-sequencing data, Fisher's exact test was used to determine statistical significance between Venn diagram overlap genes. For lifespan and survival analysis, the OASIS2 software (https://sbi.postech.ac.kr/oasis2/) was used to calculate mean lifespan, 95% confidence interval, and statistical significance between conditions using the Log-rank test (Han *et al.* 2016). For all statistical tests $^{*}P < 0.05$, $^{**}P < 0.01$, and $^{***}P < 0.001$, false discovery rate (FDR) correction was used for all *P*-values involving RNA-sequence datasets.

Results

Reduced protein translation inhibits cadmium-induced alternative splicing

Exposure to environmental stress are known to inhibit pre-mRNA splicing (Biamonti and Caceres 2009). We recently showed that the heavy metal cadmium can alter RNA splicing in *C. elegans*, potentially by disrupting the snRNA processing function of the Integrator complex (Wu *et al.* 2019). To obtain a visual biomarker to study cadmium-induced alternative splicing, we used an in vivo fluorescent alternative splicing reporter constructed with the *C. elegans ret-1* gene (Kuroyanagi *et al.* 2013). Briefly, this *C. elegans* splicing reporter strain expresses a pair of integrated fluorescent *ret-1* minigenes driven by the ubiquitous *eft-3* promoter. The mCherry reporter is modified with a +1 nucleotide insertion to exon 5, while the GFP reporter is modified with +1 insertion to exon 5 and +2 insertion to exon 6 (Fig. 1a). The nucleotide insertions alter the native reading frame of each fluorescent reporter, resulting in mCherry fluorescence when exon 5 is skipped or GFP fluorescence when exon 5 is included (Kuroyanagi *et al.* 2013; Heintz *et al.* 2017). Using this splicing reporter, we show that exposure to 300 µM of cadmium for 24 h results in a strong loss of GFP fluorescence in the intestinal tissue, indicating an increased incidence of exon 5 skipping (Fig. 1b). We did not observe noticeable changes to mCherry fluorescence that is primarily expressed in the nervous system and body wall muscle, this may be due to potential differences in cadmium presence in these tissues compared to the intestine that is the primary site of xenobiotic bioaccumulation and the major tissue of the *C. elegans* heavy metal stress response (Girard *et al.* 2007). As such, we focused specifically on changes to the GFP fluorescence as an indicator for cadmium-induced splicing alterations for this study.

To verify alternative splicing occurs to the endogenous *ret-1* gene, we exposed wild-type worms with 0, 100, 200, and 300 µM of cadmium followed by RNA extraction and RT-PCR analysis with primer pairs that bind to exon 4 and exon 6 of the endogenous *ret-1* gene (Heintz *et al.* 2017). Two isoforms of the *ret-1* transcript are amplified and can be visualized via agarose gel electrophoresis, with the top band representing the full *ret-1* transcript expressing exons 4, 5, and 6, and the bottom band representing the skipped *ret-1* transcript expressing only exons 4 and 6 (Fig. 1c). Exposure to incremental concentration of cadmium increased the relative proportion of the bottom band representing the skipped isoform. The effects of cadmium on *ret-1* alternative splicing appears to be stronger in the splicing reporter compared to RT-PCR. The relative variance may be attributed by the fact that GFP fluorescence in the splicing reporter is primarily expressed in the intestine tissue while RT-PCR measured the endogenous splicing patterns of *ret-1* using whole worm RNA samples. As such, the effects of cadmium on *ret-1* alternative splicing may be stronger in the intestine compared to the whole animal.

We then performed a genome-wide RNAi screen to identify genetic regulators of cadmium-induced alternative splicing (Fig. 1d). We screened ∼19,000 dsRNA clones and identified 74 gene knockdowns that resulted in the retention of the *ret-1* GFP reporter fluorescence after cadmium exposure. Using DAVID functional analysis, we found a strong enrichment for protein translation processes among the 74 positive hits from the RNAi screen (Fig. 1e), with the majority of the RNAi targeting genes encoding small or large ribosomal proteins and various protein translation initiating factors (Supplementary Table 1). Interestingly, secondary confirmation screen revealed that knockdown of several genes encoding translation factors reduced GFP fluorescence under basal conditions compared to the EV control. However, all candidate genes tested also resulted in the retention of GFP fluorescence after cadmium exposure relative to the EV control (Fig. 1f). Overall, these findings revealed that suppression of protein translation inhibits cadmium-induced alternative splicing.

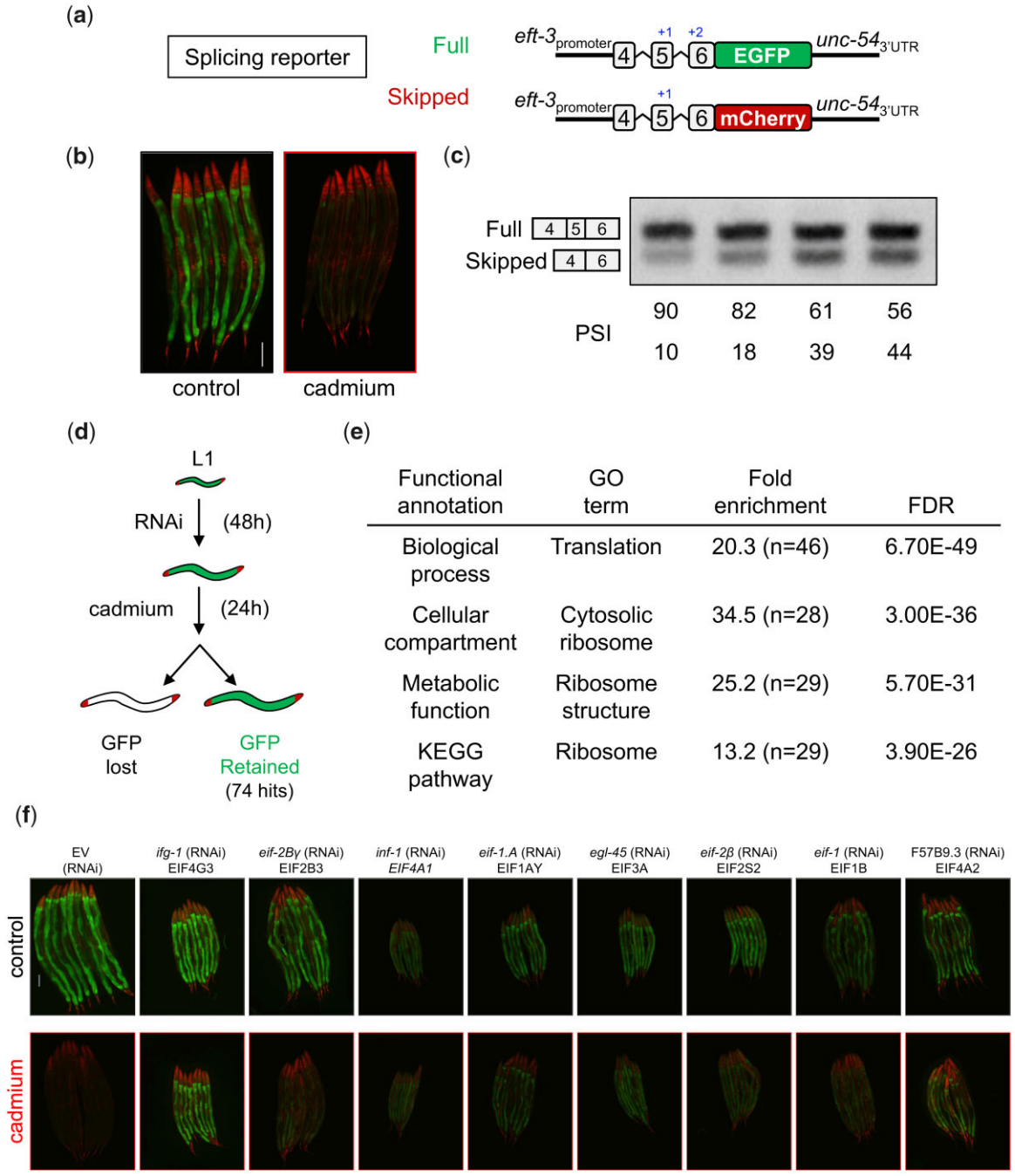

Fig. 1. Suppression of protein translation inhibits cadmium-induced exon skipping. a) Schematic representation of the in vivo splicing reporter expressing a pair of modified *ret-1* minigenes fused to EGFP or mCherry (modified from Kuroyanagi *et al.* 2013; Heintz *et al.* 2017). b) Representative images of the splicing reporter under control conditions and after cadmium exposure. Scale bar = 100 μm. c) Representative RT-PCR gel image of the relative ratio of skipped/full-length endogenous *ret-1* isoform after 0, 100, 200, and 300 μM of cadmium. Percentage spliced in index is shown below each gel band. d) Workflow of the genome-wide RNAi screen. A complete list of RNAi hits is shown in Supplementary Table 1. e) DAVID enrichment analysis of genes encoding the 74 dsRNA clones that resulted in *ret-1* GFP retention after cadmium exposure. f) Representative images of *ret-1* fluorescence in worms fed with dsRNA targeting translation initiation genes before and after cadmium exposure. Scale bar = 100 μm.

Suppression of *ifg-1* enhances *C. elegans* survival

It is well established that reducing protein synthesis via depletion of various translation-related genes extends lifespan in *C. elegans* (Hansen *et al.* 2007; Pan *et al.* 2007). We selected 4 genes from the RNAi screened that demonstrated high retention of *ret-1* GFP reporter fluorescence after cadmium exposure to determine their role in lifespan and cadmium resistance regulation. These 4 genes were also chosen as they function at different steps of protein translation including ribosomal structural protein, translation initiation factor, and ribosome biogenesis process. RNAi depletion initiated at day 1 of adulthood of *rps-23* (human homolog: ribosome protein S23) and *ifg-1* (human homolog: eIF4G) extended mean lifespan in all 3 independent trials whereas knockdown of F57B9.3 (human homolog: eIF4A2) and Y61A9LA.10 (human homolog: BMS1 ribosome biogenesis factor) extended mean lifespan in 2 out of 3 trials (Fig. 2a). Interestingly, only RNAi depletion to *ifg-1* and *rps-23* led to a consistent significant increase in cadmium survival relative to EV control (Fig. 2b).

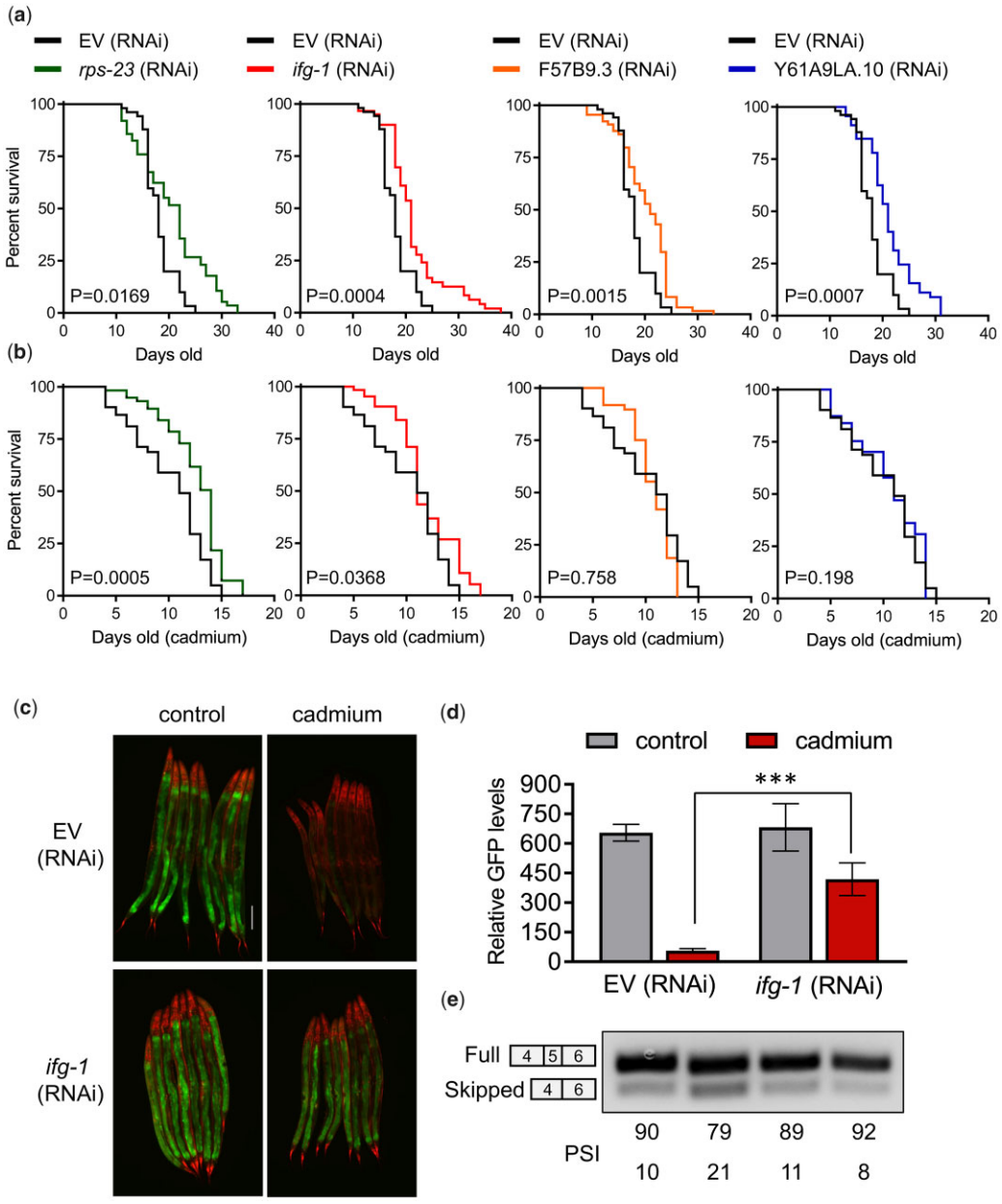

Fig. 2. Reduced expression of *ifg-1* increases *C. elegans* survival. a) Lifespan and b) cadmium survival of worms after *rps-23*, *ifg-1*, F57B9.3, and Y61A9LA.10 RNAi initiated at day one of adulthood. Trial 1 is shown for the lifespan curves, and trial 3 is shown for cadmium survival curves. Three independent trials were performed for each assay. Detailed statistics for individual trials are shown in Supplementary Table 2. c) Representative image and d) quantification of *ret-1* fluorescence between EV and *ifg-1* RNAi fed worms before and after cadmium exposure. $N = 4$ images, each containing 8 worms for a total of 32 worms analyzed per condition. $P < 0.001$ as determined via 2-way ANOVA. e) Representative gel image and percentage spliced in (PSI) index of the endogenous *ret-1* gene in wild-type and *ifg-1(cxTi9279)* mutant worms before and after cadmium exposure.

Knockdown of *rps-23* increased mean survival by an average of 12.9% under normal conditions and by 43.4% under cadmium. Meanwhile, knockdown of *ifg-1* had a smaller variation with a mean survival increase of 17.8% under normal condition and an increase of 23.5% under cadmium (Supplementary Table 2). The variable effect on cadmium survival suggests that knockdown of different translation regulators may invoke distinct downstream signals, which may include an overlapping effect on longevity but not stress survival. We decided to focus our downstream analysis on *ifg-1* given that its knockdown produced the strongest inhibition to cadmium-induced alternative splicing (Fig. 1f) and consistently extended *C. elegans* survival under normal and cadmium conditions (Fig. 2, a and b).

Given that RNAi from the genome-wide screen was initiated at the L1 stage, knockdown of *ifg-1* resulted in the larval arrest of *C. elegans* at the L2/L3 stage. To verify that knockdown of *ifg-1* inhibition against cadmium-induced *ret-1* alternative splicing is not due to RNAi-induced developmental delay, we first attempted to introduce a viable *ifg-1(cxTi9279)* partial loss of function mutation background into the *ret-1* splicing reporter strain (Morrison *et al.* 2014); however, we were not able to recover viable homozygous offspring (data not shown). Given that the *ret-1* splicing reporter has been shown to gradually lose a substantial amount of GFP fluorescence as early as 5 days old through aging (Heintz *et al.* 2017), it restricts the comparison of cadmium-induced reduction in GFP fluorescence to only young worms. To minimize

developmental differences between EV and *ifg-1* RNAi within an age window where *ret-1* GFP is highly fluorescent, we initiated RNAi depletion of *ifg-1* at the L2/L3 stage for 48 h followed by 24 h of cadmium exposure. This ensured that comparisons were made when worms are 2 days old where *ret-1* GFP is still highly expressed. Worms with *ifg-1* depleted via RNAi at L2/L3 were able to reach adulthood and retained high levels of *ret-1* GFP fluorescence after cadmium exposure compared to the EV control (Fig. 2, c and d). To verify that alternative splicing changes are also observed to the endogenous *ret-1* transcript, we extracted total RNA from wild-type and *ifg-1(cxTi9279)* worms with and without cadmium treatment. RT-PCR analysis showed that cadmium exposure increased the skipped/full ratio of the *ret-1* transcript in the wild type, and this ratio remained unchanged in the *ifg-1(cxTi9279)* mutant (Fig. 2e). Overall, these findings revealed that reduction of protein translation via depletion of *ifg-1* increases *C. elegans* resistance to cadmium and confers inhibition against cadmium-induced alternative splicing.

The transcriptome of *ifg-1* mutant resembles a cadmium-induced stress response

To investigate how reduced *ifg-1* expression protects against cadmium toxicity, we first analyzed transcription changes in wild-type and *ifg-1(cxTi9279)* worms treated with and without cadmium by whole-transcriptome RNA sequencing (Fig. 3a). RNA-sequencing revealed that *ifg-1(cxTi9279)* worms show a 57% reduction in the *ifg-1* mRNA level (Fig. 3b), indicating that this partial loss of function mutant derives from decreased transcript abundance. This reduction is comparable to a previous study demonstrating a 42% decrease in *ifg-1* mRNA in this mutant as determined via Northern blot (Morrison *et al.* 2014). The *ifg-1(cxTi9279)* worms displayed a dramatically altered transcriptome compared to the wild type, with 1,423 up-regulated genes and 4,246 down-regulated genes (>2-fold change, $P_{adj} < 0.05$ Supplementary Table 3). KEGG pathway analysis revealed that *ifg-1(cxTi9279)* up-regulated genes enriched to antioxidant stress response pathways and protein metabolism, while down-regulated genes enriched to pathways regulating neuroactivity along with calcium and Wnt signaling pathways (Fig. 3c). Up-regulation of stress response genes in *ifg-1* depleted worms was similarly demonstrated previously through translation state array analysis, which showed an increased abundance of stress genes associated with highly translated ribosome fractions (Rogers *et al.* 2011).

A clustered heat map analysis demonstrated that gene expression changes to the *ifg-1(cxTi9279)* mutant were highly similar to wild type after cadmium exposure (Fig. 3d). Genes that were up-regulated in both *ifg-1(cxTi9279)* mutant and wild type after cadmium exposure enrich to metabolic functions and KEGG pathways involved in antioxidant detoxification, including cytochrome P450 metabolism, glutathione activity, and ABC transporters. Meanwhile, genes down-regulated in both conditions enrich to metabolic enzyme functions including endopeptidase inhibitor and hydrolase (Fig. 3d). For cadmium-induced gene expression changes greater than 2-fold, linear regression analysis revealed a highly significant ($P < 0.001$) Pearson correlation coefficient of +0.65 when compared to expression changes to the same genes in the translation compromised *ifg-1(cxTi9279)* mutant (Fig. 3e). Previous studies have shown that suppression of protein synthesis is commonly observed in response to cellular stress as an adaptive mechanism to maintain proteostasis (Harding *et al.* 2003). Consistently, a previous study in human cells showed that exposure to cadmium inhibits protein synthesis (Ovelgönne *et al.* 1995). These results suggest that mutations to *ifg-1(cxTi9279)* mimic a state of cadmium stress at the transcriptome level and that the overlap in gene expression changes between *ifg-1(cxTi9279)* and cadmium may both be in response to attenuated translation efficiency.

Cadmium-induced alternative splicing is modified in the *ifg-1* mutant

Through RNA-sequencing, we next compared the transcriptome-wide alternative splicing of the *ifg-1(cxTi9279)* mutant relative to wild type worms treated with cadmium. This is accomplished by first determining the inclusion level (IncLevel) of a given transcript that is defined as a ratio between 2 alternatively spliced transcript isoforms detected (Fig. 4a), followed by calculating their relative differences between the experimental conditions (IncLevel difference) to determine significant alternative splicing events (Shen *et al.* 2014). Cadmium exposure in wild type worms resulted in 437 significant alternative splicing events, 209 of these events were not significantly different in the *ifg-1(cxTi9279)* mutant (Fig. 4b). This indicated that *ifg-1* mutants showed a 48% decrease in significant cadmium-induced alternative splicing events observed in the wild type. RNA-seq data also showed that cadmium treated *ifg-1(cxTi9279)* mutants significantly increased *ret-1* exon 5 inclusion compared to the wild type by ∼18% (*ifg-1* IncLevel = 0.673 ± 0.039, WT = IncLevel 0.569 ± 0.012; Supplementary Table 3), supporting the results obtained from the splicing reporter and RT-PCR (Fig. 2, c–e). Next, we performed a linear regression analysis of IncLevel difference between cadmium treated *ifg-1(cxTi9279)* and cadmium treated wild type for the 437 alternative splicing events. This analysis revealed a negative Pearson correlation of −0.37 ($P < 0.001$), resulting from majority of the data points positioned within the upper left and lower right quadrant where alternative splicing events occurs in the reverse direction in the *ifg-1(cxTi9279)* mutant relative to the wild type under cadmium (Fig. 4c). This suggested that the relative degree of cadmium-induced alternative splicing changes observed in wild type worms is diminished in the *ifg-1(cxTi9279)* mutant. Correlation analysis for each alternative splicing type revealed that while 4 out of 5 categories showed a negative correlation coefficient, only exon skipping and alternative 3′ splice site (A3SS) coefficients are statistically significant (Supplementary Fig. 1). It should be noted that exon skipping and A3SS account for 73% of all alternative splicing events induced by cadmium (320/437), and the lack of statistical significance may be due to a relatively small number of splicing events in other categories.

Next, we analyzed the relative percentage of intron and intergenic reads between the wild-type and *ifg-1(cxTi9279)* mutant. Given that the cDNA sequencing library was constructed with poly-A capture enrichment, these 2 parameters are indicators of aberrant splicing and have previously been shown to increase with age and after spliceosome inhibition (Heintz *et al.* 2017). In the *ifg-1(cxTi9279)* mutant, the relative percentage of both intron reads and intergenic reads are significantly lower compared to the wild type, suggesting that alternative splicing is augmented in the *ifg-1 (cxTi9279)* mutant (Fig. 4d).

Functional analysis of the 209 genes accounting for 48% of cadmium-induced alternative splicing observed in the wild type that are not significantly altered in the *ifg-1(cxTi9279)* mutant revealed enrichment toward biological functions related to muscle contraction and cell adhesion located within the actin cytoskeleton cellular compartments (Fig. 4e). No enrichment to KEGG pathway was observed likely due to the small number of genes. Given that cadmium-induced alternative splicing of genes functioning in

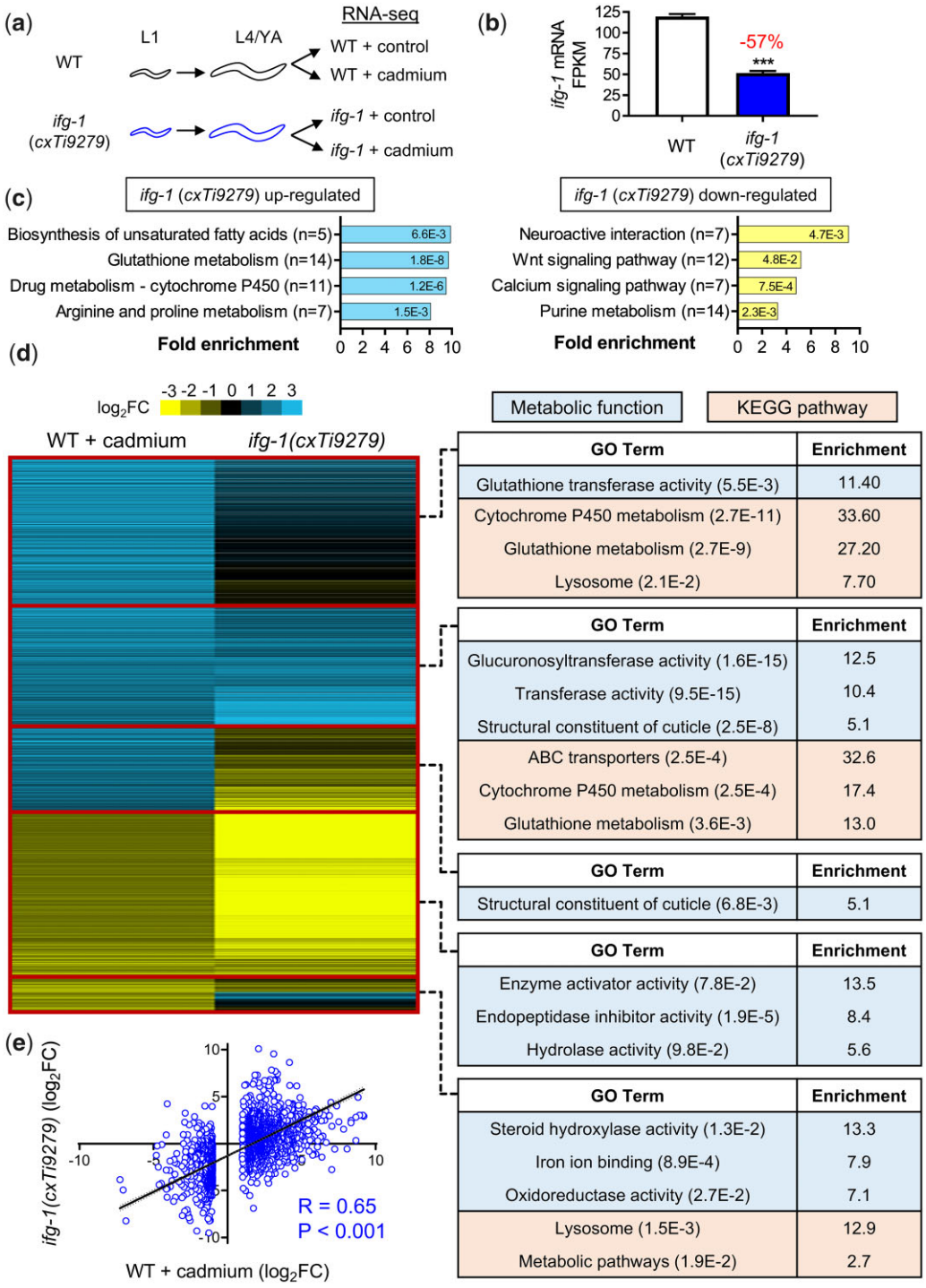

Fig. 3. RNA-sequencing reveals transcriptome similarities between wild type cadmium exposure and *ifg-1* mutant. a) Experimental workflow for RNA extraction for transcriptome sequencing. b) FPKM values of *ifg-1* mRNA in wild type (WT) and *ifg-1(cxTi9279)* mutant. Mean values are graphed with error bars representing standard deviation of the mean; $N = 3$ replicates with each RNA sample obtained from ~2,000–3,000 worms, $^{***}P < 0.001$ as determined via student t-test. c) KEGG pathway enrichment of gene up or down-regulated by >2-fold (FDR < 0.05) in the *ifg-1(cxTi9279)* mutant. FDR values are included within each bar. d) Heat map of differentially expressed genes in WT + cadmium and *ifg-1(cxTi9279)* mutant worms cluster by relative expression change; all genes were differentially expressed by >2-fold (FDR < 0.05). DAVID enrichment analysis of genes within each heat map segment based on relative similarity or difference in expression between WT + cadmium and *ifg-1(cxTi9279)* mutant. Enriched metabolic function and KEGG pathways are shown with FDR values included in brackets. e) Linear regression analysis of genes with >2-fold change (FDR < 0.05) in WT + cadmium compared to the expression of the corresponding genes in the *ifg-1(cxTi9279)* mutant. R indicates Pearson correlation value with $P < 0.001$ as determined by the linear regression *F* test.

muscle regulation, we measured the swimming behavior of wild-type and *ifg-1(cxTi9279)* mutant after 24 and 48 h of cadmium exposure. Cadmium exposure for 24 h led to a 21.8% decrease in wild-type swimming motility as determined by body bends per second, and this reduction is significantly improved in the *ifg-1(cxTi9279)* mutant where only a 10.9% decrease was observed

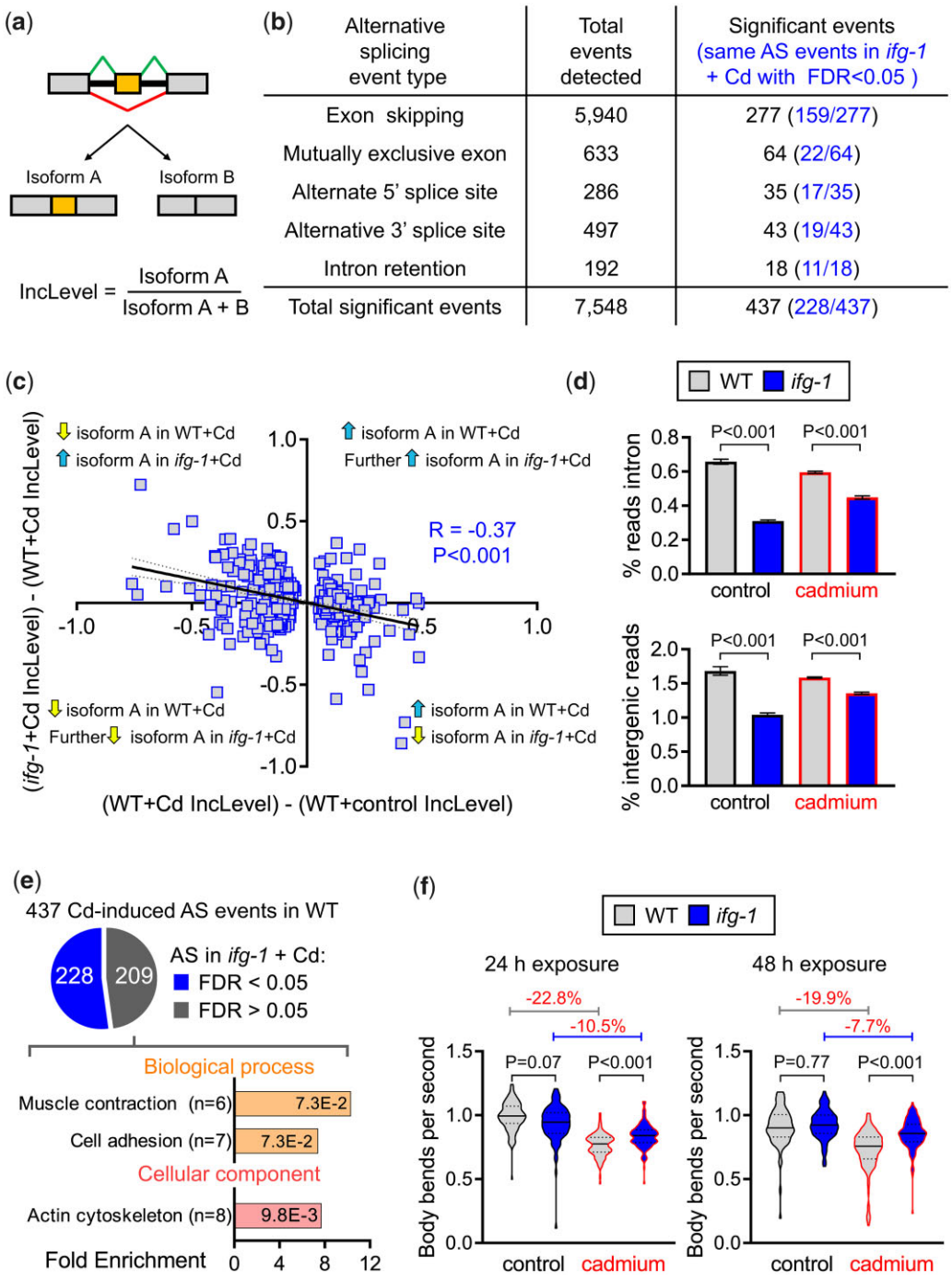

Fig. 4. *ifg-1* mutant inhibits cadmium-induced alternative splicing. a) Schematic example of exon skipping event producing 2 transcript isoforms used to calculate inclusion level by rMATS, adapted from (Shen *et al.* 2014). b) The number of alternative splicing events detected in wild type (WT) worms after cadmium exposure categorized by different event types. Same alternative splicing events were evaluated for statistical significance in *ifg-1(cxTi9279)* worms after cadmium exposure and presented in brackets. c) Linear regression analysis of inclusion level difference between *ifg-1(cxTi9279)* and WT for the 437 significant alternative splicing events detected in cadmium exposed WT worms. d) Percentage of intron and intergenic region reads in WT and *ifg-1(cxTi9279)* before and after cadmium exposure. Mean values are graphed with error bars representing standard deviation of the mean; $N = 3$ replicates with each RNA sample obtained from ~2,000–3,000 worms, statistical significance was determined by the 2-way ANOVA test. e) DAVID enrichment analysis of 209 genes not alternatively spliced in *ifg-1(cxTi9279)* after cadmium exposure. Enriched biological processes and cellular compartments are shown with FDR values included within each bar. f) Swim motility of WT and *ifg-1(cxTi9279)* worms after 24 or 48 h cadmium treatment. Mean values are graphed with error bars representing the standard deviation of the mean. $N = 89$–130 worms scored for 24 h and 77–140 worms for 48 h in each condition, combined from 2 independent trials. The 2-way ANOVA test determined statistical significance.

after cadmium exposure (Fig. 4f). Similar trends were also observed after 48 h cadmium exposure. It should be noted these experiments only show an association of improved motility in the *ifg-1* mutant under cadmium, as it was not determined in this study whether cadmium-induced alternative splicing of transcripts related to muscle functions are directly detrimental to motility. Together, these results revealed that cadmium-induced alternative splicing observed in wild type worms are reduced in

the *ifg-1(cxTi9279)* mutant and that these modifications may provide resistance against cadmium-induced impairment to muscle functions.

SMA transcription factors regulate *ifg-1*-mediated gene expressions

To gain mechanistic insights on how reduced *ifg-1* provides inhibition against cadmium-induced alternative splicing, we performed a small-scale RNAi screen to identify transcription factors that are required to maintain *ret-1* GFP fluorescence after *ifg-1* depletion and cadmium exposure. The rationale for this approach is that potential transcription factors may act downstream of reduced *ifg-1* to modulate RNA splicing via changes to gene expression. We first initiated *ifg-1* depletion via RNAi in L2/L3 worms for 48 h, followed by feeding with ∼500 dsRNA clones targeting *C. elegans* transcription factors for another 48 h before treatment with cadmium (Fig. 5a). In *ifg-1*-depleted worms subsequently fed with EV RNAi as a control, we show that these worms are able to maintain high GFP fluorescence after cadmium exposure (Fig. 5b). This suggested that a secondary RNAi treatment did not reduce the penetrance of the initial *ifg-1* depletion. Using this protocol, we identified 2 dsRNA clones corresponding to the *sma-2* and *sma-3* genes that suppressed *ifg-1* induced retention of *ret-1* GFP following cadmium exposure (Fig. 5b). Quantitative analysis revealed that knockdown of *sma-2* after *ifg-1* depletion resulted in a significant decrease of GFP levels after cadmium exposure, which was unchanged in *ifg-1* depleted worms fed with EV control. While knockdown of *sma-3* also reduced GFP levels after cadmium exposure, the decrease was not statistically significant. This may be attributed by *sma-3* knockdown causing a significant reduction in GFP levels under basal conditions compared to the EV control, thereby reducing the relative difference in GFP levels after cadmium exposure (Fig. 5b). The *C. elegans* *sma-2* and *sma-3* encode receptor-regulated Smad proteins within the TGF-β/BMP signaling pathway that was initially characterized for its role in body size regulation (Savage *et al.* 1996; Savage-Dunn and Padgett 2017). Given the defined role of SMA proteins functioning as transcription factors, we compared the transcriptome of a *sma-2(rax5)* mutant previously described with a defect in lipid metabolism to the transcriptome of the *ifg-1(cxTi9279)* mutant from this study (Yu *et al.* 2017). We observed a striking overlap between genes that are up-regulated in the *ifg-1(cxTi9279)* mutant but down-regulated in the *sma-2(rax5)* mutant (FDR > 0.05, no FC cut-off) (Fig. 5c), with 79% (2,899/3,680) of genes down-regulated in the *sma-2(rax5)* mutant found to be up-regulated in the *ifg-1(cxTi9279)* mutant. Functional analysis of the 2,899 overlapped genes revealed enrichment toward RNA metabolism pathways including RNA transport and the spliceosome (Fig. 5d). Other KEGG pathways enriched include proteasome, nucleotide excision repair, and ER processing. We then analyzed the 2 RNA-sequencing datasets and manually identified 88 genes functioning in various processes in RNA splicing regulation that were up-regulated (1.2- to 1.9-fold) in the *ifg-1(cxTi9279)* mutant but down-regulated in the *sma-2(rax5)* mutant (Fig. 5e and Supplementary Table 4).

To further examine the relationship between *ifg-1* and *sma-2*, we performed linear regression analysis on the expression of 12,114 genes that are differentially expressed (FDR < 0.05) in the *ifg-1(cxTi9279)* mutant against their corresponding expression in the *sma-2(rax5)* mutant and observed a Pearson correlation coefficient of −0.27 ($P < 0.001$) (Fig. 5f). Reciprocal analysis of 5,840 genes differentially expressed in the *sma-2(rax5)* mutant also revealed similar patterns with a Pearson correlation coefficient of −0.41 ($P < 0.001$) (Fig. 5g). While no RNA-sequencing data was available for a *sma-3* mutant, similar results were also observed when comparing the transcriptome of a *sma-4(rax3)* mutant to the *ifg-1(cxTi9279)* mutant showing an overlap of 3,699 genes (Supplementary Fig. 2a). Consistently, linear regression analysis on gene expression data between the 2 mutants revealed a Pearson correlation coefficient of −0.39 ($P < 0.001$) and −0.52 ($P < 0.001$) when *ifg-1(cxTi9279)* or *sma-4(rax3)* differentially expressed genes were analyzed respectively (Supplementary Fig. 2, b and c).

To further investigate the relationship between *ifg-1* and *sma* genes, we found that transcript levels of *sma-2*, *sma-3*, and *sma-4* genes are all up-regulated in response to cadmium, and this response is further enhanced in the *ifg-1(cxTi9279)* mutant compared to the wild type (Supplementary Fig. 3, a–c). This suggests that the *ifg-1* mutant positively promotes the expression of *sma* encoding genes as a potential mechanism to influence the transcription of *sma* dependent splicing regulatory genes. Interestingly, in both the *sma-2(rax5)* and *sma-4(rax3)* mutants, transcript levels of *ifg-1* are significantly decreased by 24% and 29%, respectively, compared to the wild type (Supplementary Fig. 3d and Supplementary Table 5). This reduction in *ifg-1* mRNA level is comparable to that observed in the *ifg-1(cxTi9279)* mutant (Fig. 3b) and potentially explains the significant transcriptome overlap of reciprocal changes between the *ifg-1(cxTi9279)* mutant to the *sma-2(rax5)* and *sma-4(rax3)* mutants (Fig. 5c and Supplementary Fig. 2a). Overall, our results demonstrated that knockdown of *sma-2* suppressed *ifg-1(cxTi9279)*-mediated inhibition toward cadmium-induced alternative splicing, which may be attributed to the requirement for *sma-2* in regulating transcription of RNA splicing regulatory genes that are up-regulated in the *ifg-1(cxTi9279)* mutant.

Core RNA-splicing regulatory genes are required for *ifg-1* longevity and stress resistance

Our data suggest that *sma* and RNA-splicing factors function downstream of reduced *ifg-1*. To test this, we used RNAi to knockdown *sma-2*, *sma-3*, and 4 RNA splicing regulatory genes that were up-regulated in the *ifg-1(cxTi9279)* mutant and down-regulated in either the *sma-2(rax5)* or *sma-4(rax3)* mutant to determine their effects on wild type and *ifg-1(cxTi9279)* lifespan and stress resistance. We had attempted to generate an *ifg-1;sma-2* double mutant but the combination of these 2 mutations appears to be synthetic lethal as no homozygous worms carrying both mutations could be recovered (data not shown). The mean lifespan of *ifg-1(cxTi9279)* is significantly increased by ∼25% compared to the wild type; this is consistent with previous reports (Fig. 6a and Supplementary Tables 6 and 7) (Pan *et al.* 2007; Rogers *et al.* 2011). Knockdown of *sma-2* and *sma-3* slightly reduced *ifg-1(cxTi9279)* lifespan by 7% and 8%, respectively (Fig. 6, a and b; $P < 0.05$ in 2/3 trials for *sma-2* and 3/3 trials for *sma-3*; Supplementary Table 6), but did not reduce the lifespan of wild type worms. Consistent with our *ifg-1* RNAi data (Fig. 2b), the *ifg-1* mutant also shows increased resistance against cadmium compared to the wild type; however, knockdown of either *sma-2* or *sma-3* did not reduce this resistance (Fig. 6, a and b and Supplementary Table 8). This suggests that *sma-2* and *sma-3* are not required for the *ifg-1* cadmium survival and is consistent with previous evidence demonstrating that *ifg-1* confers its stress resistance phenotype largely via activation of stress response genes dependent on the transcription factor *skn-1* (Wang *et al.* 2010).

We next investigated whether 4 RNA-splicing regulatory genes up-regulated in the *ifg-1(cxTi9279)* mutant are required for its longevity and stress-resistant phenotypes. RNAi knockdown of small

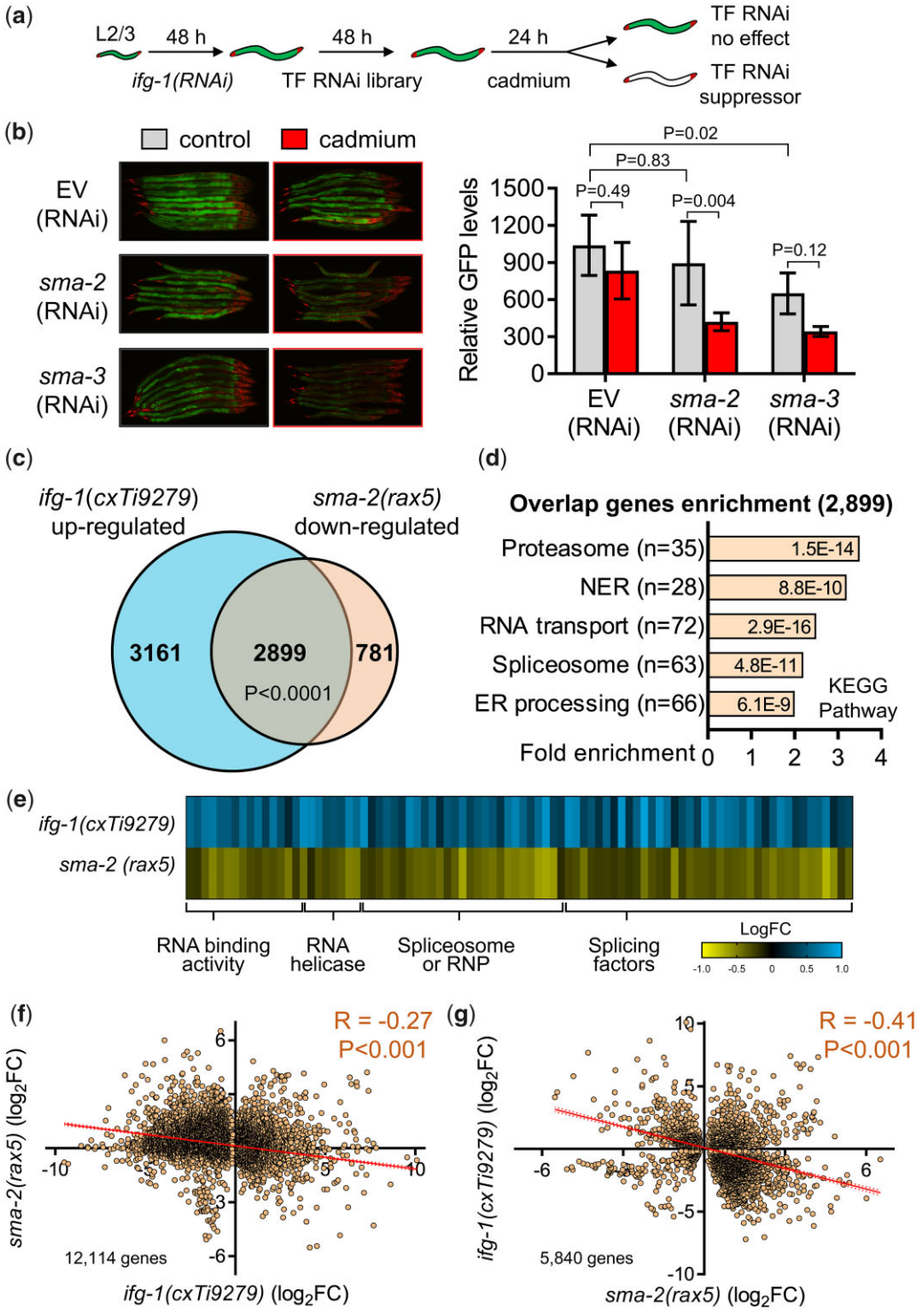

Fig. 5. *sma* regulates transcription of genes altered in the *ifg-1* mutant. a) Workflow of the transcription factor sub-library RNAi screen. b) Quantification and representative image of *ret-1* fluorescence between EV, *sma-2*, and *sma-3* RNAi fed worms before and after cadmium exposure. Mean values are graphed with error bars representing the standard deviation of the mean. $N = 4$ images, each containing 8 worms for a total of 32 worms analyzed per condition. The 2-way ANOVA test determined statistical significance. c) Venn diagram illustrating number of genes overlapping between *ifg-1(cxTi9279)* up-regulated and *sma-2(rax5)* down-regulated conditions. $P < 0.001$ as determined by Fisher's exact test. Raw transcriptome data for *sma-2(rax5)* were obtained from (Yu *et al.* 2017). d) KEGG pathway enrichment of overlapped genes between *ifg-1(cxTi9279)* up-regulated and *sma-2(rax5)* down-regulated conditions. FDR values are included within each bar. e) Heat map of 88 RNA splicing regulatory genes significantly up-regulated in *ifg-1(cxTi9279)* and down-regulated in *sma-2(rax5)* mutants. f) Linear regression analysis of fold change for genes differentially expressed in *ifg-1(cxTi9279)* compared to its corresponding fold change in *sma-2(rax5)*. g) Linear regression analysis of fold change for genes differentially expressed in *sma-2(rax5)* compared to its corresponding fold change in *ifg-1(cxTi9279)*. R indicates Pearson correlation value with $P < 0.001$ as determined by the linear regression *F* test.

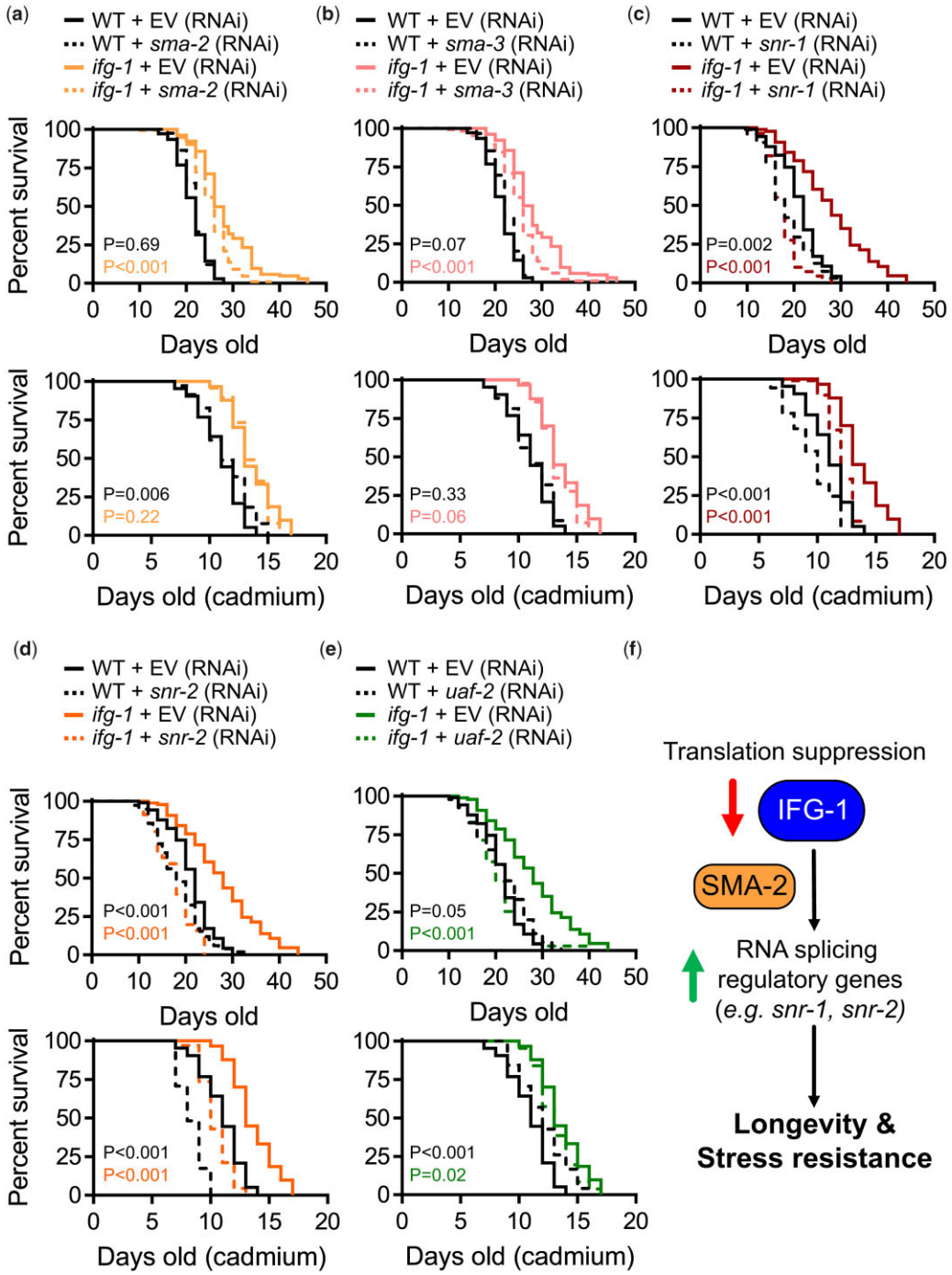

Fig. 6. Core RNA splicing regulator genes are required for the longevity and stress resistance of the *ifg-1* mutant. Lifespan and cadmium resistance of wild type (WT) and *ifg-1(cxTi9279)* mutant worms after a) *sma-2* (RNAi), b) *sma-3* (RNAi), c) *snr-1* (RNAi), d) *snr-2* (RNAi), and e) *uaf-2* (RNAi) knockdown. *P*-values are shown comparing the treatment RNAi with EV control in colored fonts that correspond to either the WT or the *ifg-1(cxTi9279)* mutant. Three independent trials were performed for each assay; detailed statistics for individual trials are shown in Supplementary Tables 6–8. Trial 1 is shown for longevity assay, and trial 2 is shown for cadmium survival. f) Model of proposed regulation between *ifg-1*- and *sma-2*-dependent RNA-splicing factors in the longevity and stress resistance phenotype of the *ifg-1* mutant.

nuclear ribonucleoproteins *snr-1* and *snr-2* beginning at day 1 of adulthood significantly reduced wild type lifespan by an average of 15.8% and 18.5%, respectively, and completely nullified the long-lived phenotype of the *ifg-1(cxTi9279)* mutant with *snr-1* RNAi causing a 27.2% decrease and *snr-2* RNAi causing a 33.2% decrease in mean lifespan (Fig. 6, c and d and Supplementary Tables 7 and 8). Similarly, knockdown of both *snr-1* and *snr-2* significantly reduced the stress resistance of the wild type worms by an average of 10.5% and 22.6%, respectively, and in the *ifg-1(cxTi9279)* mutant by an average of 7.5% and 25.6%, respectively (Fig. 6, c and d and Supplementary Tables 7 and 8). Interestingly, knockdown of the U2 small nuclear RNA auxiliary factor *uaf-2* beginning at day 1 of adulthood also completely nullified *ifg-1(cxTi9279)* mutant's long-lived lifespan (22% decrease in mean lifespan) but did not affect the wild type lifespan (Fig. 6e and Supplementary Tables 7 and 8). Knockdown of *uaf-2* also did

not decrease stress resistance of the wild type worms and slightly reduced the *ifg-1(cxTi9279)* mutant stress resistance in 1 out of 3 trials (Fig. 6e and Supplementary Tables 7 and 8). Meanwhile, RNAi knockdown of the serine arginine-rich protein *rsp-2* did not affect either the wild type or *ifg-1(cxTi9279)* mutant lifespan or stress resistance (Supplementary Fig. 4 and Supplementary Tables 7 and 8). Together, these results show that the extent to which different splicing factors are required for *ifg-1* longevity and stress resistance are variable, and core spliceosomal encoding genes such as *snr-1* and *snr-2* that have a direct influence on transcriptome-wide splicing dynamics and gene expression regulation are completely essential for the longevity and stress-resistant phenotypes of the *ifg-1(cxTi9279)* mutant.

Discussion

RNA splicing is an essential step in regulating eukaryotic gene expression and is a major contributor to transcriptome and proteome diversity (Dutertre *et al.* 2011). Aberrant RNA splicing is an underlying factor in many human diseases, including cancer and neurodegeneration (Tollervey *et al.* 2011; Scotti and Swanson 2016; Deschênes and Chabot 2017). Recently, it was demonstrated that RNA splicing deteriorates with age in *C. elegans*, suggesting a causative link between RNA splicing homeostasis and healthy aging (Heintz *et al.* 2017). To date, only a handful of studies have examined the effects of environmental stress on RNA splicing homeostasis (Yost and Lindquist 1986; Biamonti and Caceres 2009; Dutertre *et al.* 2011; Wu *et al.* 2019), and molecular mechanisms that inhibit stress-induced alternative splicing have not yet been described. Here, we show that protein translation suppression in *C. elegans* via reduced *ifg-1* influences cadmium-induced alternative splicing (Figs. 1–4), and we propose that this mechanism signals through the SMA family of transcription factors to regulate the expression of RNA splicing regulatory genes in influencing alternative splicing to promote longevity and stress resistance (Figs. 5 and 6g).

Environmental stress-induced alternative splicing

In response to stress, it is well established that cells can mount an adaptive response such as transcription of damage repair genes to elicit cellular protection. These responses can include up-regulation of chaperone genes to facilitate protein folding in response to heat stress or an increase in expression of xenobiotic detoxification genes in response to oxidative stress (An *et al.* 2005; Brunquell *et al.* 2016). However, the functional significance of stress-induced alternative splicing is not well understood, as modifications to transcript splicing could indicate an adaptive response or as a consequence of pathological events. Evidence for stress-induced alternative splicing with detrimental consequences has been reported in response to heat stress, where widespread alternative splicing of ~1,700 genes is observed in the mouse fibroblast that is associated with the impaired translation of the alternatively spliced transcripts (Shalgi *et al.* 2014). We previously showed that cadmium exposure alters the Integrator complex's function, resulting in the aberrant polyadenylation and misprocessing of several snRNA transcripts that normally assemble with ribonucleoproteins in forming a functional spliceosome (Matera *et al.* 2007; Baillat and Wagner 2015; Wu *et al.* 2019). Disruption of the Integrator complex in *C. elegans* is deleterious and impairs RNA splicing leading to widespread transcriptome dysregulation (Gómez-Orte *et al.* 2019). RNAi knockdown of the Integrator complex via subunit-4 depletion results in embryonic lethality and produces an alternative splicing profile that is significantly correlated to the alternative splicing pattern observed after cadmium exposure (Wu *et al.* 2019). While these evidence do not rule out the possibility that some of the cadmium-induced alternative splicing events are an adaptive response, the resemblance in alternative splicing events between Integrator dysfunction and cadmium exposure suggest that cadmium-induced alternative splicing events may also be deleterious.

Influence of translational suppression on RNA splicing and aging

It is well established that reduced protein translation via mutation or knockdown of various ribosomal and translation factors can significantly extend lifespan in worm, fly, and yeast (Kapahi *et al.* 2004; Kaeberlein *et al.* 2005; Hansen *et al.* 2007; Pan *et al.* 2007; Curran and Ruvkun 2007; Steffen *et al.* 2008; Zid *et al.* 2009; Rogers *et al.* 2011). Mechanistically, a conserved cellular response to reduced protein translation includes the selective up-regulation and increased translation of various genes involved in stress signaling (Zid *et al.* 2009; Rogers *et al.* 2011). Consistently, suppression of protein translation in worms provides enhanced resistance to various environmental stress including hypoxia, thermotolerance, oxidative stress, heavy metal stress, and ER stress (Anderson *et al.* 2009; Wang *et al.* 2010; Howard *et al.* 2016). The mechanism behind lifespan extension induced by protein translation suppression is likely to be multifactorial, given that transcriptome-wide alteration to gene expression is observed (Fig. 3), and presumably, to the proteome as well. It is hypothesized that the combination of enhanced stress resistance and global reduction to protein translation both contribute to the longevity phenotype (Steffen and Dillin 2016). Enhanced stress resistance may provide an increase in cellular repair response to mitigate the progressive buildup of molecular damage accumulated through aging (Gems and Partridge 2013). Our results show that the *ifg-1* mutant up-regulates various stress-responsive genes involved in xenobiotic detoxification (Fig. 3). This is consistent with a previous report showing enhanced oxidative stress resistance in *ifg-1* depleted worms, which is dependent on the SKN-1 transcription factor that functions as a master regulator of antioxidant defense (An *et al.* 2005; Wang *et al.* 2010; Wu *et al.* 2017). Interestingly, while loss of *skn-1* abolishes *ifg-1*'s oxidative stress resistance, it had minimal impact on its longevity (Wang *et al.* 2010), suggesting that enhanced oxidative stress response may not be the primary factor in promoting longevity in translation compromised mutants.

Meanwhile, reduced translation may directly decelerate the proposed hypertrophic effect of protein synthesis in later life, which is supported by evidence that translation fidelity decreases with age leading to an increase in the accumulation of translational errors (Gems and Partridge 2013; Anisimova *et al.* 2018). Mild inhibition of translation has also been shown to increase protein folding accuracy in mammalian cells, suggesting a positive effect of reduced translation on enhancing overall protein synthesis fidelity (Meriin *et al.* 2012). Similar to translation, RNA splicing efficiency also declines with age, a deterioration that can be protected through dietary restriction in *C. elegans* (Heintz *et al.* 2017). In this study, we provide evidence that translation inhibition via reduced *ifg-1* also modifies RNA splicing; however, this may be accomplished via independent mechanisms compared to dietary restriction that did not show global changes to splicing factor mRNA expression (Fig. 5e). Expression of splicing regulators is a determinant factor in mouse and human longevity (Lee *et al.* 2016), and down-regulation of splicing factors is observed

with increasing chronological age in men (Holly et al. 2013). In calorically restricted Rhesus monkeys that lived on average 20% longer than the control group, transcriptome analysis of liver biopsy samples showed up-regulation of various components of the spliceosome (Rhoads et al. 2018). Though it should be cautioned that the correlative relationship between splicing factor expression and aging likely differs between organisms and can vary across different tissues, and functional studies are required to determine their relative contribution to aging. In this study, we showed that different splicing factors had varying effects on *C. elegans* lifespan and stress resistance. Depleting *rsp-2* encoding an SR protein had no effect on either the lifespan or stress resistance whereas knockdown of *snr-1* and *snr-2* encoding core spliceosome proteins reduced both of these phenotypes in the wild type and *ifg-1* mutant worms. Furthermore, knockdown of *uaf-2* encoding the U2 auxiliary factor only reduced *ifg-1* lifespan but not the wild type. It should be noted that a previous study that introduced *uaf-2* RNAi beginning at the L1 stage instead of day 1 adulthood used in this study showed a significant reduction in wild type lifespan (Heintz et al. 2017). These data suggest a differential requirement of splicing factors in lifespan and stress resistance regulation that is dependent on both the genetic background and expression during development.

Why does translational suppression influence RNA splicing? Under periods of environmental stress, cells naturally cope by suppressing global protein translation via eIF2α phosphorylation (Wek et al. 2006). This allows cells to redirect energy resources to prioritize other essential needs, including enhancing RNA processing to limit the potential stress-induced disruption to RNA splicing. While cells can protect against mis-spliced mRNA molecules via RNA surveillance mechanisms such as nonsense-mediated decay (NMD), costs associated with degradation of an erroneous transcript is energetically expensive given that it costs at least 10 ATP molecules to perform splicing of each intron and that NMD relies on the activity of various ATP-dependent hydrolysis reactions (Lynch and Marinov 2015; Serdar et al. 2016). Modifications to RNA splicing may also prevent the translation of erroneous transcripts that can cost on average 100–200 molecules of ATP to degrade (Peth et al. 2013; Lynch and Marinov 2015). Given that the combined energetic cost of RNA transcription and splicing are magnitudes lower than the cost of protein translation and degradation, these modifications may ensure the production of accurate mature transcripts before translation to avoid loss of energy investment toward the synthesis and degradation of aberrant proteins.

SMA signaling in aging

TGF-β/Sma signaling is a critical developmental pathway in *C. elegans* initially discovered for its role in regulating body size growth and male tail morphogenesis (Savage et al. 1996; Savage-Dunn and Padgett 2017). In the last decade, a role for TGF-β/Sma signaling in aging has also been described. Loss of function mutations to *sma* genes delay reproductive aging characterized by an extended offspring production window supported by improved oocyte and germline quality (Luo et al. 2009, 2010). In the oocyte of *sma-2* mutants, reproductive aging is delayed via transcriptional up-regulation of genes involved in cell cycle regulation, DNA damage repair, and cell death programming, while down-regulating genes involved in oviposition, proteolysis, and cell differentiation (Luo et al. 2010). Recently, a role for SMA in regulating lipid metabolism has also been described, with *sma-2* and *sma-4* mutants transcriptionally up-regulating various β-oxidation genes to reduce lipid storage in *C. elegans* (Yu et al. 2017; Clark et al. 2018). These transcriptional programs appear to be distinct from the regulation of genes involved in RNA metabolism described in this study, suggesting a pleiotropic role for the TGF-β/Sma signaling in regulating diverse cellular functions. Our study shows that depletion of either *sma-2* or *sma-3* does not shorten wild type lifespan but partially reduces the longevity of the *ifg-1* mutant. This suggests a differential requirement of *sma* genes in influencing lifespan that is dependent on the genetic background, where SMA may function as critical transcription factors in long-lived mutants to regulate the expression of genes required to potentiate longevity. This genotype-specific requirement for *sma* genes in longevity was also recently demonstrated in an insulin signaling mutant where loss *sma-3* partially reduced the longevity of the *daf-2(e1370)* worms (Clark et al. 2021).

In summary, we have described a new mechanism through which suppression of protein translation provides inhibition against stress-induced alternative splicing in *C. elegans*. We show that reducing the translation initiation factor *ifg-1* up-regulates the expression of RNA splicing regulators and inhibits stress-induced alternative splicing. Overall, these findings reveal novel mechanistic insights into RNA splicing regulation under stress and highlight its importance in promoting longevity and stress resistance.

Data availability

All datasets supporting this manuscript are found within the article and its supplementary files. RNA-sequencing data generated from this study (raw and annotated) are available on the NCBI GEO data repository GSE184491. Strains are available upon request.

Supplemental material is available at *GENETICS* online.

Acknowledgments

Some *C. elegans* strains were provided by the *Caenorhabditis* Genetic Centre (University of Minnesota, Minneapolis, MN, USA), which is supported by the NIH Office of Research Infrastructure Programs (P40 OD010440). We thank Dr. Hidehito Kuroyanagi (Tokyo Medical and Dental University) for providing the KH2235 strain and Dr. Brett Keiper (East Carolina University) for providing the *ifg-1(cxTi9279)* strain.

Funding

C.-W.W. is supported by an Natural Sciences and Engineering Research Council of Canada (NSERC) Discovery Grant (04486) and an Saskatchewan Health Research Foundation (SHRF) Establishment Grant (4971). S.C.C. and H.T. were supported by a Western College of Veterinary Medicine (WCVM) graduate teaching fellowship award.

Author contributions

S.C.C. and H.T. performed the experiments and S.C.C. analyzed the results. C.-W.W. designed the study, performed experiments, and analyzed results. C.-W.W. and S.C.C. wrote the manuscript.

Conflicts of interest

None declared.

Literature cited

Afgan E, Baker D, Batut B, van den Beek M, Bouvier D, Cech M, Chilton J, Clements D, Coraor N, Grüning BA, *et al.* The Galaxy platform for accessible, reproducible and collaborative biomedical analyses: 2018 update. Nucleic Acids Res. 2018;46(W1):W537–W544.

An JH, Vranas K, Lucke M, Inoue H, Hisamoto N, Matsumoto K, Blackwell TK. Regulation of the *Caenorhabditis elegans* oxidative stress defense protein SKN-1 by glycogen synthase kinase-3. Proc Natl Acad Sci U S A. 2005;102(45):16275–16280.

Anders S, Huber W. Differential expression analysis for sequence count data. Genome Biol. 2010;11(10):R106–12.

Anderson LL, Mao X, Scott BA, Crowder CM. Survival from hypoxia in *C. elegans* by inactivation of aminoacyl-tRNA synthetases. Science. 2009;323(5914):630–633.

Anisimova AS, Alexandrov AI, Makarova NE, Gladyshev VN, Dmitriev SE. Protein synthesis and quality control in aging. Aging (Albany NY). 2018;10(12):4269–4288.

Baillat D, Wagner EJ. Integrator: urprisingly diverse functions in gene expression. Trends Biochem Sci. 2015;40(5):257–264.

Baralle FE, Giudice J. Alternative splicing as a regulator of development and tissue identity. Nat Rev Mol Cell Biol. 2017;18(7):437–451.

Biamonti G, Caceres JF. Cellular stress and RNA splicing. Trends Biochem Sci. 2009;34(3):146–153.

Brenner S. The genetics of *Caenorhabditis elegans*. Genetics. 1974;77(1):71–94.

Brunquell J, Morris S, Lu Y, Cheng F, Westerheide SD. The genome-wide role of HSF-1 in the regulation of gene expression in *Caenorhabditis elegans*. BMC Genomics. 2016;17:559.

Clark JF, Meade M, Ranepura G, Hall DH, Savage-Dunn C. *Caenorhabditis elegans* DBL-1/BMP regulates lipid accumulation via interaction with insulin signaling. G3 (Bethesda). 2018;8(1):343–351.

Clark JF, Ciccarelli EJ, Kayastha P, Ranepura G, Yamamoto KK, Hasan MS, Madaan U, Meléndez A, Savage-Dunn C. BMP pathway regulation of insulin signaling components promotes lipid storage in *Caenorhabditis elegans*. PLoS Genet. 2021;17(10):e1009836.

Curran SP, Ruvkun G. Lifespan regulation by evolutionarily conserved genes essential for viability. PLoS Genet. 2007;3(4):e56.

Deschênes M, Chabot B. The emerging role of alternative splicing in senescence and aging. Aging Cell. 2017;16(5):918–933.

Dutertre M, Sanchez G, Barbier J, Corcos L, Auboeuf D. The emerging role of pre-messenger RNA splicing in stress responses: sending alternative messages and silent messengers. RNA Biol. 2011;8(5):740–747.

Eskens FALM, Ramos FJ, Burger H, O'Brien JP, Piera A, de Jonge MJA, Mizui Y, Wiemer EAC, Carreras MJ, Baselga J, *et al.* Phase I pharmacokinetic and pharmacodynamic study of the first-in-class spliceosome inhibitor E7107 in patients with advanced solid tumors. Clin Cancer Res. 2013;19(22):6296–6304.

Felkai S, Ewbank JJ, Lemieux J, Labbé JC, Brown GG, Hekimi S. CLK-1 controls respiration, behavior and aging in the nematode *Caenorhabditis elegans*. EMBO J. 1999;18(7):1783–1792.

Feng J, Bussière F, Hekimi S. Mitochondrial electron transport is a key determinant of life span in *Caenorhabditis elegans*. Dev. Cell. 2001;1(5):633–644.

Gems D, Partridge L. Genetics of longevity in model organisms: debates and paradigm shifts. Annu Rev Physiol. 2013;75:621–644.

Girard LR, Fiedler TJ, Harris TW, Carvalho F, Antoshechkin I, Han M, Sternberg PW, Stein LD, Chalfie M. WormBook: the online review of Caenorhabditis elegans biology. Nucleic Acids Res. 2007;35(Database issue):D472–D475.

Gómez-Orte E, Sáenz-Narciso B, Zheleva A, Ezcurra B, de Toro M, López R, Gastaca I, Nilsen H, Sacristán MP, Schnabel R, *et al.* Disruption of the *Caenorhabditis elegans* integrator complex triggers a non-conventional transcriptional mechanism beyond snRNA genes. PLoS Genet. 2019;15(2):e1007981.

Hansen M, Taubert S, Crawford D, Libina N, Lee S-J, Kenyon C. Lifespan extension by conditions that inhibit translation in *Caenorhabditis elegans*. Aging Cell. 2007;6(1):95–110.

Harding HP, Zhang Y, Zeng H, Novoa I, Lu PD, Calfon M, Sadri N, Yun C, Popko B, Paules R, *et al.* An integrated stress response regulates amino acid metabolism and resistance to oxidative stress. Mol. Cell. 2003;11(3):619–633.

Heintz C, Doktor TK, Lanjuin A, Escoubas CC, Zhang Y, Weir HJ, Dutta S, Silva-García CG, Bruun GH, Morantte I, *et al.* Splicing factor 1 modulates dietary restriction and TORC1 pathway longevity in *C. elegans*. Nature. 2017;541(7635):102–106.

Holly AC, Melzer D, Pilling LC, Fellows AC, Tanaka T, Ferrucci L, Harries LW. Changes in splicing factor expression are associated with advancing age in man. Mech Ageing Dev. 2013;134(9):356–366.

Howard AC, Rollins J, Snow S, Castor S, Rogers AN. Reducing translation through eIF4G/IFG-1 improves survival under ER stress that depends on heat shock factor HSF-1 in *Caenorhabditis elegans*. Aging Cell. 2016;15(6):1027–1038.

Huang DW, Sherman BT, Lempicki RA. Systematic and integrative analysis of large gene lists using DAVID bioinformatics resources. Nat Protoc. 2009;4(1):44–57.

Kaeberlein M, Powers RW, Steffen KK, Westman EA, Hu D, Dang N, Kerr EO, Kirkland KT, Fields S, Kennedy BK, *et al.* Regulation of yeast replicative life span by TOR and Sch9 in response to nutrients. Science. 2005;310(5751):1193–1196.

Kapahi P, Zid BM, Harper T, Koslover D, Sapin V, Benzer S. Regulation of lifespan in Drosophila by modulation of genes in the TOR signaling pathway. Curr Biol. 2004;14(10):885–890.

Kenyon C, Chang J, Gensch E, Rudner A, Tabtiang R. A *C. elegans* mutant that lives twice as long as wild type. Nature. 1993;366(6454):461–464.

Han SK, Lee D, Lee H, Kim D, Son HG, Yang J-S, Lee S-JV, Kim S. OASIS 2: online application for survival analysis 2 with features for the analysis of maximal lifespan and healthspan in aging research. Oncotarget. 2016;7(35):56147–56152.

Kim D, Paggi JM, Park C, Bennett C, Salzberg SL. Graph-based genome alignment and genotyping with HISAT2 and HISAT-genotype. Nat Biotechnol. 2019;37(8):907–915.

Kuroyanagi H, Watanabe Y, Suzuki Y, Hagiwara M. Position-dependent and neuron-specific splicing regulation by the CELF family RNA-binding protein UNC-75 in *Caenorhabditis elegans*. Nucleic Acids Res. 2013;41(7):4015–4025.

Lee BP, Pilling LC, Emond F, Flurkey K, Harrison DE, Yuan R, Peters LL, Kuchel GA, Ferrucci L, Melzer D, *et al.* Changes in the expression of splicing factor transcripts and variations in alternative splicing are associated with lifespan in mice and humans. Aging Cell. 2016;15(5):903–913.

Luo S, Shaw WM, Ashraf J, Murphy CT. TGF-ß Sma/Mab signaling mutations uncouple reproductive aging from somatic aging. PLoS Genet. 2009;5(12):e1000789.

Luo S, Kleemann GA, Ashraf JM, Shaw WM, Murphy CT. TGF-β and insulin signaling regulate reproductive aging via oocyte and germline quality maintenance. Cell. 2010;143(2):299–312.

Lynch M, Marinov GK. The bioenergetic costs of a gene. Proc Natl Acad Sci U S A. 2015;112(51):15690–15695.

Matera AG, Terns RM, Terns MP. Non-coding RNAs: lessons from the small nuclear and small nucleolar RNAs. Nat Rev Mol Cell Biol. 2007;8(3):209–220.

Meriin AB, Mense M, Colbert JD, Liang F, Bihler H, Zaarur N, Rock KL, Sherman MY. A novel approach to recovery of function of mutant proteins by slowing down translation. J Biol Chem. 2012;287(41): 34264–34272.

Morrison JK, Friday AJ, Henderson MA, Hao E, Keiper BD. 2014. Induction of cap-independent BiP (hsp-3) and Bcl-2 (ced-9) translation in response to eIF4G (IFG-1) depletion in *C. elegans*. Translation. 2: e28935.

Murray SM, Waddell BM, Wu CW. Neuron-specific toxicity of chronic acrylamide exposure in *C. elegans*. Neurotoxicol Teratol. 2020;77: 106848.

Nilsen TW, Graveley BR. Expansion of the eukaryotic proteome by alternative splicing. Nature. 2010;463(7280):457–463.

Nussbaum-Krammer CI, Neto MF, Brielmann RM, Pedersen JS, Morimoto RI. Investigating the spreading and toxicity of prion-like proteins using the metazoan model organism *C. elegans*. JoVE. 2015;(95):e52321.

Ovelgönne JH, Souren JEM, Wiegant FAC, Van Wijk R. Relationship between cadmium-induced expression of heatshock genes, inhibition of protein synthesis and cell death. Toxicology. 1995; 99(1–2):19–30.

Pan KZ, Palter JE, Rogers AN, Olsen A, Chen D, Lithgow GJ, Kapahi P. Inhibition of mRNA translation extends lifespan in *Caenorhabditis elegans*. Aging Cell. 2007;6(1):111–119.

Peth A, Nathan JA, Goldberg AL. The ATP costs and time required to degrade ubiquitinated proteins by the 26S proteasome. J Biol Chem. 2013;288(40):29215–29222.

Rhoads TW, Burhans MS, Chen VB, Hutchins PD, Rush MJP, Clark JP, Stark JL, McIlwain SJ, Eghbalnia HR, Pavelec DM, *et al.* Caloric restriction engages hepatic RNA processing mechanisms in rhesus monkeys. Cell Metab. 2018;27(3):677–688.e5.

Robida-Stubbs S, Glover-Cutter K, Lamming DW, Mizunuma M, Narasimhan SD, Neumann-Haefelin E, Sabatini DM, Blackwell TK. TOR signaling and rapamycin influence longevity by regulating SKN-1/Nrf and DAF-16/FoxO. Cell Metab. 2012;15(5):713–724.

Rogers AN, Chen D, McColl G, Czerwieniec G, Felkey K, Gibson BW, Hubbard A, Melov S, Lithgow GJ, Kapahi P, *et al.* Life span extension via eIF4G inhibition is mediated by posttranscriptional remodeling of stress response gene expression in *C. elegans*. Cell Metab. 2011;14(1):55–66.

Savage-Dunn C, Padgett RW. The TGF-β family in *Caenorhabditis elegans*. Cold Spring Harb. Perspect. Biol. 2017;9:

Savage C, Das P, Finelli AL, Townsend SR, Sun CY, Baird SE, Padgett RW. *Caenorhabditis elegans* genes sma-2, sma-3, and sma-4 define a conserved family of transforming growth factor beta pathway components. Proc Natl Acad Sci U S A. 1996;93(2):790–794.

Schneider CA, Rasband WS, Eliceiri KW. NIH image to ImageJ: 25 years of image analysis. Nat. Methods. 2012;9(7):671–675.

Scotti MM, Swanson MS. RNA mis-splicing in disease. Nat Rev Genet. 2016;17(1):19–32.

Serdar LD, Whiteside DL, Baker KE. ATP hydrolysis by UPF1 is required for efficient translation termination at premature stop codons. Nat. Commun. 2016;7:14021.

Shalgi R, Hurt JA, Lindquist S, Burge CB. Widespread inhibition of posttranscriptional splicing shapes the cellular transcriptome following heat shock. Cell Rep. 2014;7(5):1362–1370.

Shen S, Park JW, Lu Z-x, Lin L, Henry MD, Wu YN, Zhou Q, Xing Y. rMATS: robust and flexible detection of differential alternative splicing from replicate RNA-Seq data. Proc Natl Acad Sci U S A. 2014;111(51):E5593–601.

Steffen KK, MacKay VL, Kerr EO, Tsuchiya M, Hu D, Fox LA, Dang N, Johnston ED, Oakes JA, Tchao BN, *et al.* Yeast life span extension by depletion of 60S ribosomal subunits is mediated by Gcn4. Cell. 2008;133(2):292–302.

Steffen KK, Dillin A. A ribosomal perspective on proteostasis and aging. Cell Metab. 2016;23(6):1004–1012.

Tollervey JR, Wang Z, Hortobágyi T, Witten JT, Zarnack K, Kayikci M, Clark TA, Schweitzer AC, Rot G, Curk T, *et al.* Analysis of alternative splicing associated with aging and neurodegeneration in the human brain. Genome Res. 2011;21(10):1572–1582.

Wang ET, Sandberg R, Luo S, Khrebtukova I, Zhang L, Mayr C, Kingsmore SF, Schroth GP, Burge CB. Alternative isoform regulation in human tissue transcriptomes. Nature. 2008;456(7221):470–476.

Wang J, Robida-Stubbs S, Tullet JMA, Rual J-F, Vidal M, Blackwell TK. RNAi screening implicates a SKN-1-dependent transcriptional response in stress resistance and longevity deriving from translation inhibition. PLoS Genet. 2010;6(8):e1001048.

Wek RC, Jiang H-Y, Anthony TG. Coping with stress: eIF2 kinases and translational control. Biochem Soc Trans. 2006;34(Pt 1):7–11.

Wu CW, Deonarine A, Przybysz A, Strange K, Choe KP. The Skp1 homologs SKR-1/2 are required for the *Caenorhabditis elegans* SKN-1 antioxidant/detoxification response independently of p38 MAPK. PLoS Genet. 2016;12(10):e1006361.

Wu C-W, Wang Y, Choe KP. F-Box protein XREP-4 is a new regulator of the oxidative stress response in *Caenorhabditis elegans*. Genetics. 2017;206(2):859–871.

Wu C-W, Wimberly K, Pietras A, Dodd W, Atlas MB, Choe KP. RNA processing errors triggered by cadmium and integrator complex disruption are signals for environmental stress. BMC Biol. 2019;17(1):56.

Yost HJ, Lindquist S. RNA splicing is interrupted by heat shock and is rescued by heat shock protein synthesis. Cell. 1986;45(2):185–193.

Yu Y, Mutlu AS, Liu H, Wang MC. High-throughput screens using photo-highlighting discover BMP signaling in mitochondrial lipid oxidation. Nat. Commun. 2017;8(1):1–11.

Zid BM, Rogers AN, Katewa SD, Vargas MA, Kolipinski MC, Lu TA, Benzer S, Kapahi P. 4E-BP extends lifespan upon dietary restriction by enhancing mitochondrial activity in *Drosophila*. Cell. 2009; 139(1):149–160.

Communicating editor: J. Claycomb